

Detect RNA and protein  
simultaneously in  
millions of single cells

excellence

| Learn more >

affymetrix  
eBioscience



## **Bacillus Calmette–Guérin (BCG) Revaccination of Adults with Latent *Mycobacterium tuberculosis* Infection Induces Long-Lived BCG-Reactive NK Cell Responses**

This information is current as  
of July 15, 2016.

Sara Suliman, Hennie Geldenhuys, John L. Johnson, Jane E. Hughes, Erica Smit, Melissa Murphy, Asma Toefy, Lesedi Lerumo, Christiaan Hopley, Bernadette Pienaar, Phalkun Chheng, Elisa Nemes, Daniel F. Hoft, Willem A. Hanekom, W. Henry Boom, Mark Hatherill and Thomas J. Scriba

*J Immunol* published online 13 July 2016  
<http://www.jimmunol.org/content/early/2016/07/13/jimmunol.1501996>

**Supplementary Material** <http://www.jimmunol.org/content/suppl/2016/07/13/jimmunol.1501996.DCSupplemental.html>

**Subscriptions** Information about subscribing to *The Journal of Immunology* is online at:  
<http://jimmunol.org/subscriptions>

**Permissions** Submit copyright permission requests at:  
<http://www.aai.org/ji/copyright.html>

**Email Alerts** Receive free email-alerts when new articles cite this article. Sign up at:  
<http://jimmunol.org/cgi/alerts/etoc>

*The Journal of Immunology* is published twice each month by  
The American Association of Immunologists, Inc.,  
9650 Rockville Pike, Bethesda, MD 20814-3994.  
Copyright © 2016 by The American Association of  
Immunologists, Inc. All rights reserved.  
Print ISSN: 0022-1767 Online ISSN: 1550-6606.



# Bacillus Calmette–Guérin (BCG) Revaccination of Adults with Latent *Mycobacterium tuberculosis* Infection Induces Long-Lived BCG-Reactive NK Cell Responses

Sara Suliman,\* Hennie Geldenhuys,\* John L. Johnson,<sup>†</sup> Jane E. Hughes,\* Erica Smit,\* Melissa Murphy,\* Asma Toefy,\* Lesedi Lerumo,\* Christiaan Hopley,\* Bernadette Pienaar,<sup>\*,1</sup> Phalkun Chheng,<sup>†</sup> Elisa Nemes,\* Daniel F. Hoft,<sup>‡</sup> Willem A. Hanekom,\* W. Henry Boom,<sup>†</sup> Mark Hatherill,<sup>\*,2</sup> and Thomas J. Scriba<sup>\*,2</sup>

One third of the global population is estimated to be latently infected with *Mycobacterium tuberculosis*. We performed a phase I randomized controlled trial of isoniazid preventive therapy (IPT) before revaccination with bacillus Calmette–Guérin (BCG) in healthy, tuberculin skin test–positive ( $\geq 15$ -mm induration), HIV-negative South African adults. We hypothesized that preclearance of latent bacilli with IPT modulates BCG immunogenicity following revaccination. Frequencies and coexpression of IFN- $\gamma$ , TNF- $\alpha$ , IL-2, IL-17, and/or IL-22 in CD4 T cells and IFN- $\gamma$ -expressing CD8 T,  $\gamma\delta$  T, CD3<sup>+</sup>CD56<sup>+</sup> NKT-like, and NK cells in response to BCG were measured using whole blood intracellular cytokine staining and flow cytometry. We analyzed 72 participants who were revaccinated with BCG after IPT ( $n = 33$ ) or without prior IPT ( $n = 39$ ). IPT had little effect on frequencies or cytokine coexpression patterns of *M. tuberculosis*- or BCG-specific responses. Revaccination transiently boosted BCG-specific Th1 cytokine-expressing CD4, CD8, and  $\gamma\delta$  T cells. Despite high frequencies of IFN- $\gamma$ -expressing BCG-reactive CD3<sup>+</sup>CD56<sup>+</sup> NKT-like cells and CD3<sup>-</sup>CD56<sup>dim</sup> and CD3<sup>-</sup>CD56<sup>hi</sup> NK cells at baseline, BCG revaccination boosted these responses, which remained elevated up to 1 y after revaccination. Such BCG-reactive memory NK cells were induced by BCG vaccination in infants, whereas in vitro IFN- $\gamma$  expression by NK cells upon BCG stimulation was dependent on IL-12 and IL-18. Our data suggest that isoniazid preclearance of *M. tuberculosis* bacilli has little effect on the magnitude, persistence, or functional attributes of lymphocyte responses boosted by BCG revaccination. Our study highlights the surprising durability of BCG-boosted memory NKT-like and NK cells expressing antimycobacterial effector molecules, which may be novel targets for tuberculosis vaccines. *The Journal of Immunology*, 2016, 197: 000–000.

**T**uberculosis is the leading cause of morbidity and mortality from a curable bacterial infection worldwide (1). It is estimated that one third of the global population is infected with *Mycobacterium tuberculosis* (2), placing a massive number of people at risk for subsequent tuberculosis (TB) disease. Isoniazid preventative therapy (IPT), targeted at clearing replicating *M. tuberculosis* bacilli, decreased the risk for TB disease by 60% in a combined analysis of randomized controlled trials of IPT in HIV-uninfected adults (3). However, in settings of ongoing *M. tuberculosis* transmission, efficacy of IPT may be short-lived (4), and prophylaxis is typically targeted at high-risk populations, such as young children and HIV-infected persons (5). Paradoxically, established latent *M. tuberculosis* infection (LTBI) may afford some

protection against risk for active TB disease upon subsequent reinfection in bacillus Calmette–Guérin (BCG)-naïve persons (6). The mechanisms of this protective effect are unknown, but one possibility is through maintenance of protective *M. tuberculosis* Ag-driven effector responses, as demonstrated in BCG-vaccinated mice (7). As a consequence, some investigators argued that IPT-mediated clearance of *M. tuberculosis* may remove Ag-driven immunity, rendering the person at elevated risk for reinfection with *M. tuberculosis* and at risk for TB disease. Household contacts of index TB cases reverted from positive tuberculin skin tests (TSTs) following IPT in a Ugandan cohort study (8), and decreases in *M. tuberculosis*-specific T cell responses were reported after anti-TB treatment (9) or treatment of LTBI (10). However, other studies (11–16) showed no changes or

\*South African Tuberculosis Vaccine Initiative, Institute of Infectious Disease and Molecular Medicine and Division of Immunology, Department of Pathology, University of Cape Town, Cape Town 7925, South Africa; <sup>†</sup>Tuberculosis Research Unit, Department of Medicine, Case Western Reserve University and University Hospitals Case Medical Center, Cleveland, OH 44106; and <sup>‡</sup>Division of Immunobiology, Departments of Internal Medicine and Molecular Biology, Saint Louis University Medical Center and Center for Vaccine Development, St. Louis, MO 63104

<sup>1</sup>Deceased.

<sup>2</sup>M.H. and T.J.S. contributed equally to this work.

ORCID: 0000-0002-5154-576X (S.S.); 0000-0002-2221-8997 (H.G.); 0000-0002-9534-2534 (J.E.H.); 0000-0001-9906-0713 (M.M.); 0000-0002-0437-4101 (L.L.); 0000-0002-6738-4972 (P.C.); 0000-0003-1662-4961 (E.N.); 0000-0001-5760-9595 (W.H.B.).

Received for publication September 10, 2015. Accepted for publication June 7, 2016.

This work was supported by the Tuberculosis Research Unit at Case Western Reserve University, established with funds from the National Institutes of Allergy and Infec-

tious Diseases, National Institutes of Health and Human Services under Contracts N01-A195383 and HHSN266200700022C/N01-AI-70022 and National Institutes of Health Grant R01-AI087915. S.S. is supported by Carnegie Corporation and South Africa National Research Foundation Innovation postdoctoral fellowships.

Address correspondence and reprint requests to Dr. Thomas J. Scriba, South African Tuberculosis Vaccine Initiative, Institute of Infectious Disease and Molecular Medicine and Division of Immunology, Department of Pathology, University of Cape Town, Cape Town, Western Cape 7925, South Africa. E-mail address: thomas.scriba@uct.ac.za

The online version of this article contains supplemental material.

Abbreviations used in this article: BCG, bacillus Calmette–Guérin; IBO, INH-BCG-ICS, intracellular cytokine staining; INH, isoniazid; IPT, isoniazid preventative therapy; LTBI, latent *M. tuberculosis* infection; OBI, observation-BCG-INH; rh, recombinant human; TB, tuberculosis; TST, tuberculin skin test.

Copyright © 2016 by The American Association of Immunologists, Inc. 0022-1767/16/\$30.00

even increased levels of IFN- $\gamma$  responses after IPT and/or TB treatment.

We recently completed a phase I randomized controlled trial in healthy, TST-positive HIV-negative South African adults to determine how isoniazid (INH) treatment before revaccination with BCG changed *M. tuberculosis*-specific immune responses (17). We reasoned that preclearance of latent *M. tuberculosis* bacilli by IPT would enhance specific immune responses to *M. tuberculosis* after BCG revaccination, compensating for possible waning of immunity resulting from clearance of the underlying *M. tuberculosis* infection. We previously reported that IPT had no effect on changes in QuantiFERON-TB Gold In-Tube assay results during short-term follow-up (17) and that BCG revaccination of adults with LTBI was safe and well tolerated (18).

In the current study, we performed comprehensive analyses of *M. tuberculosis* and BCG-specific CD4 and CD8 T cell responses, as well as BCG-reactive NK cells and unconventional T cells, such as CD3<sup>+</sup>CD56<sup>+</sup> (hereafter termed CD3<sup>+</sup>CD56<sup>+</sup> NKT-like) and  $\gamma\delta$  T cells, and addressed three questions. First, does INH pretreatment of adults with LTBI modulate frequencies and/or functional profiles of mycobacteria-specific immune responses? Second, can BCG revaccination boost pre-existing mycobacteria-specific responses in adults who are highly sensitized to *M. tuberculosis*? Third, does BCG revaccination induce durable changes in BCG-reactive

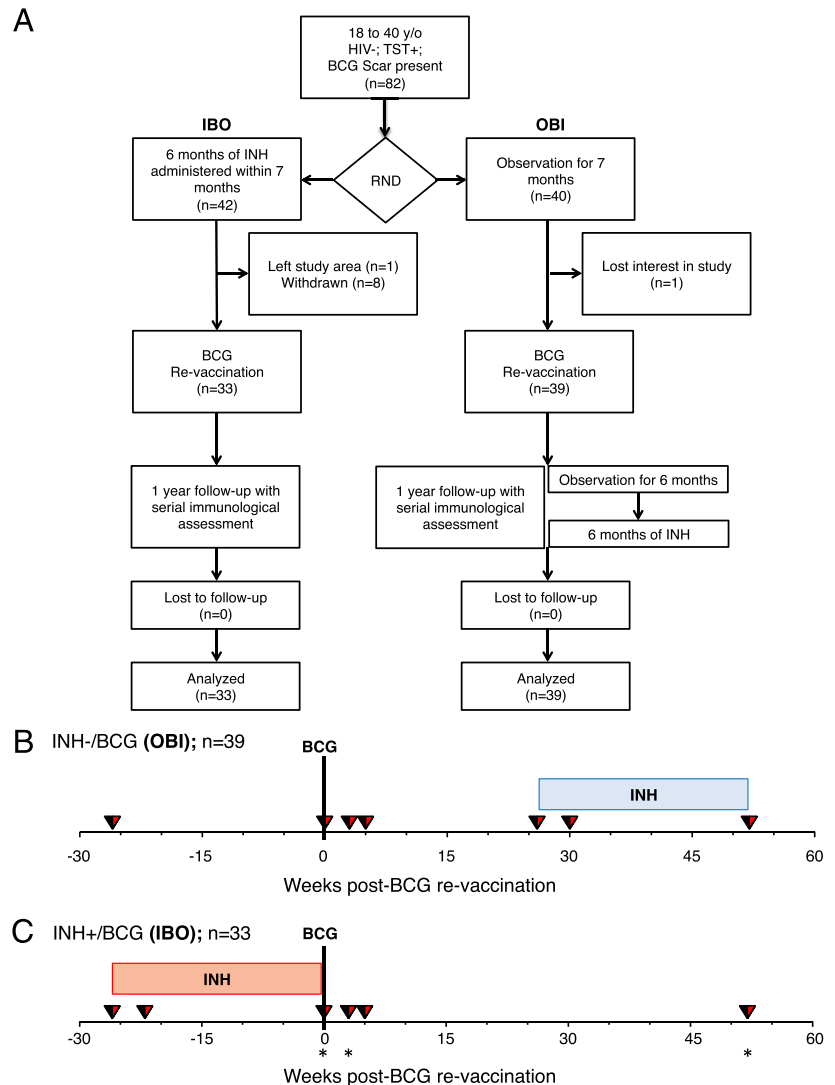
immune cells, which could potentially be targeted with whole-cell vaccines against TB?

## Materials and Methods

### Study participants and treatment groups

**BCG revaccination trial.** We recruited healthy 18–40-y-old South African adults who were strongly TST positive ( $\geq 15$ -mm induration when tested with PPD RT-23), HIV seronegative, received BCG at birth, and had a visible BCG scar. Participants were recruited from the population of Worcester in the Western Cape, South Africa, an area highly endemic for TB. In this phase I trial, participants were randomized in parallel into two groups in a 1:1 ratio (Fig. 1), as previously described (17, 18). Participants in the first group were observed for 7 mo, vaccinated with BCG, and treated with INH 6 mo later (observation-BCG-INH [OBI] group). Participants in the second group received a course of 6 mo of INH within a maximum period of 7 mo, followed by BCG vaccination, and a subsequent period of observation (INH-BCG-observation [IBO] group). Danish strain 1331 BCG Vaccine SSI (Statens Serum Institut, Copenhagen, Denmark), the BCG vaccine used in the South African national immunization program and one of the most widely administered BCG vaccines worldwide, was administered intradermally at an adult dose of  $2\text{--}8 \times 10^5$  CFU. INH (Westward Pharmaceutical, Eatontown, NJ) was administered daily at 5 mg/kg rounded up to the nearest 100 mg (maximum dose 300 mg/d), and INH adherence was monitored by pill counts at clinic visits and random urine INH metabolite testing (18). Heparinized whole blood was collected from participants and processed within 45 min of phlebotomy, as previously described (19), at enrollment, 1 mo after IPT initiation, at BCG vaccination, and at 3 and 5 wk and 1 y postvaccination (Fig. 1B, 1C).

**FIGURE 1.** (A) Consort diagram of participant recruitment and enrollment. (B and C) Study design: schematic representation of treatments, schedule of visits, and blood draws in the two groups. (B) Group receiving no INH before BCG revaccination, observed for 6 mo, and then receiving 6-mo dose of INH (in a maximum period of 7 mo) for clinical equivalence. (C) Group receiving 6-mo dose of INH, BCG revaccinated, and observed for 12 m. Blood draws for whole-blood ICS are indicated by inverted triangles for both groups. Blue and red shaded boxes correspond to when the OBI and IBO groups received IPT, respectively. Asterisks in (C) denote time points when additional experiments characterizing NK cells were performed.



**Delayed BCG vaccination study.** We performed a subanalysis of a larger delayed BCG-vaccination cohort. Pregnant mothers were contacted through public and private hospitals in Worcester, in the Western Cape, South Africa. Healthy newborns born to consenting mothers received intradermal BCG (Danish strain 1331; Statens Serum Institut) vaccine at the infant dose of  $1-4 \times 10^5$  CFU at 6 wk of age. Another cohort of healthy infants who received BCG at birth, as is routine, was recruited. Heparinized whole blood was collected at 5 wk of age from all infants, prior to administration of other routine vaccinations (and BCG in one group) scheduled at 6 wk of age.

**Healthy adult volunteer recruitment.** We recruited healthy adult volunteers > 18 y of age, who received BCG vaccination at birth. Heparinized whole blood was collected to test effects of cytokine stimulation and neutralizing Abs, as described below.

**Ethics statement**

All adult participants provided written informed consent. The protocol was approved by the Medicines Control Council of South Africa, Human Research Ethics Committee of the University of Cape Town (Ref. 387/2008), and the University Hospitals Case Medical Center institutional review board. The trial was registered at ClinicalTrials.gov (NCT01119521). Mothers of infants in the delayed BCG-vaccination cohort provided written informed consent. Human Research Ethics Committee of the University of Cape Town also approved protocols for blood collection from healthy volunteers and infants vaccinated at birth (Ref. 126/2006) and delayed BCG vaccination (Ref. 177/2011). We adhered to the World Medical Association’s Declaration of Helsinki and Good Clinical Practice guidelines during the treatment of all participants.

**AgS and whole blood intracellular cytokine staining assay**

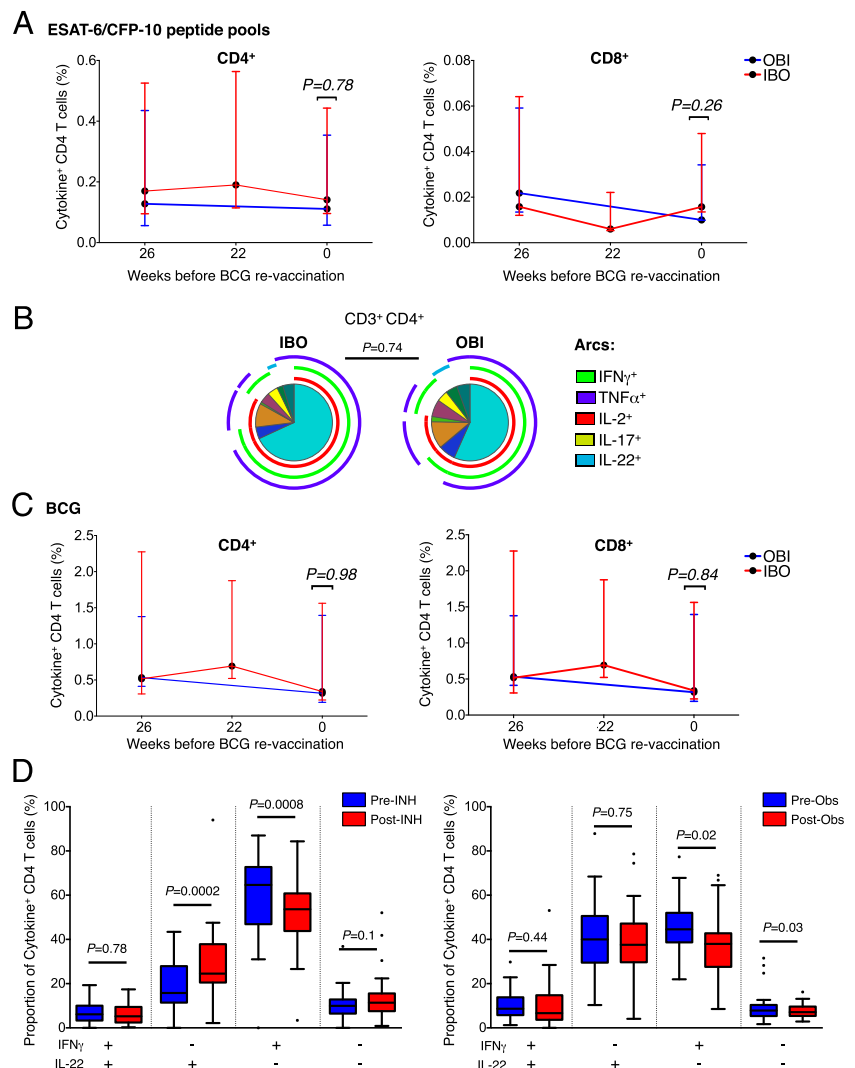
Heparinized whole blood was collected from participants and processed within 45 min of phlebotomy, as previously described (19). AgS included

BCG Vaccine SSI (Biovac, Cape Town, South Africa) reconstituted in RPMI 1640 (final concentration  $1.2 \times 10^6$  CFU/ml blood) and, in some experiments, 15-mer peptide pools spanning ESAT-6 and CFP-10 (Peptide Protein Research, London, U.K.; final concentration  $1 \mu\text{g/ml/peptide}$ ). PHA ( $5 \mu\text{g/l ml}$ ) was used as a positive mitogen control (Bioweb, Johannesburg, South Africa), and medium only was used for unstimulated negative controls. All intracellular cytokine staining (ICS) assay stimulations were performed with anti-CD28 and anti-CD49d costimulatory Abs (BD Biosciences, Mississauga, ON, Canada), each at  $0.5 \mu\text{g/ml}$  blood. Blood was stimulated at  $37^\circ\text{C}$  for a total of 12 h, and Brefeldin A (Sigma-Aldrich, St. Louis, MO) was added for the final 5 h of stimulation at  $10 \mu\text{g/ml}$ . After stimulation, blood was treated with 2 mM EDTA, RBCs were lysed with 1:10 FACS Lysing solution (BD), and fixed white cells were cryopreserved in cryosolution containing 10% DMSO, 40% FCS, and 50% RPMI 1640. For cytokine-stimulation experiments, we stimulated fresh whole blood with BCG in the ICS assay, as described above, in the presence of combinations of the following recombinant cytokines or blocking Abs at a final concentration each of  $0.1 \mu\text{g/ml}$  in whole blood: recombinant human (rh)IL-2 (BD Biosciences; catalog no. 554603), rhIL-12p70 (eBioscience, San Diego, CA; catalog no. 34-8129), or rhIL-18/IL-1F4 (R&D Systems, Minneapolis, MN; catalog no. B001-5). Neutralizing Abs included isotype controls: mouse IgG1 (clone 11711; R&D Systems), rat IgG2a (clone A110-2; R&D Systems), rat anti-human IL-2 (clone MQ1-17H12; BD Biosciences), mouse anti-human IL-12 (clone 24910; R&D Systems), and mouse anti-human IL-18 (clone 125-2H; R&D Systems). All were used at a final concentration of  $10 \mu\text{g/ml}$  in blood. The ICS assay was completed as described above.

**Abs and flow cytometry**

Cryopreserved whole-blood samples were thawed and stained at  $4^\circ\text{C}$  in BD Perm/Wash buffer (BD) with one of two Ab cocktails, described in detail in Supplemental Table I. Samples were acquired on a BD LSR II flow

**FIGURE 2.** Effect of INH on ESAT-6/CFP-10–reactive cytokine-expressing lymphocyte subsets. **(A)** Frequencies of ESAT-6/CFP-10–reactive cytokine-expressing CD4<sup>+</sup> (left panels) and CD8<sup>+</sup> (right panel) T cells. All frequencies were background subtracted. Red and blue lines denote the group treated (IBO) or not treated (OBI) with INH for 6 mo in the time window preceding BCG revaccination, respectively. No sample was collected at 22 wk before BCG revaccination in the OBI group. Unadjusted *p* values were calculated with the Mann–Whitney *U* test, comparing frequencies of cytokine-positive cells between the two groups. To correct for multiple testing (Bonferroni method), *p* values < 0.025 were considered statistically significant. **(B)** Median proportions of ESAT-6/CFP-10 peptide pool–specific CD4 T cells coexpressing IFN- $\gamma$ , TNF- $\alpha$ , IL-2, IL-17, and/or IL-22 after INH treatment (IBO) or observation (OBI). Arcs represent the cytokines expressed within each pie slice, which corresponds to cells coexpressing each cytokine combination. **(C)** Same graphs as in (A) for BCG-specific responses. **(D)** Proportions of BCG-specific CD4 T cells coexpressing IFN- $\gamma$  and/or IL-22 following INH or observation. Unadjusted *p* values were calculated with the Wilcoxon signed-rank test before and after IPT or observation. To correct for multiple testing (Bonferroni method), *p* values < 0.0125 (four comparisons) were considered statistically significant.





cytometer configured with four lasers: solid state blue (488 nm; 100 mW; three detectors), solid state violet (405 nm; 25 mW; eight detectors), HeNe gas red (635 nm; 70 mW; three detectors), and diode-pumped Coherent Compass (532 nm; 150 mW; eight detectors). Single-stained rat  $\kappa$ -chain BD CompBeads (BD Biosciences) were used to compensate APCs in the first panel, and mouse single-stained  $\kappa$ -chain BD CompBeads (BD Biosciences) for all other parameters. Samples from the same participant were batched for acquisition on the same day.

### Statistical analysis

Flow cytometry files were analyzed using FlowJo version 9.7–9.8 (TreeStar, Ashland, OR), as shown in Supplemental Fig. 1. Background subtractions were performed in Pestre version 1.7, and Boolean cytokine combinations were analyzed in SPICE version 5.3 (20). Statistical analyses were performed and graphs were created using Prism version 6 (GraphPad, La Jolla, CA). Paired longitudinal comparisons within the same group were done using the Wilcoxon signed-rank test. Comparisons across the two treatment groups were done using the Mann–Whitney  $U$  test. The  $p$  values were reported unadjusted, but were interpreted after adjustment using the Bonferroni correction for multiple comparisons.

## Results

### Enrollment and demographic characteristics

We enrolled and followed up 72 subjects randomized into IBO ( $n = 33$ ) and OBI ( $n = 39$ ) arms from October 2010 to July 2013 (Fig. 1). Baseline characteristics of the cohort were reported previously (18); there were no significant differences between the two groups with respect to age, gender, body mass index, whole

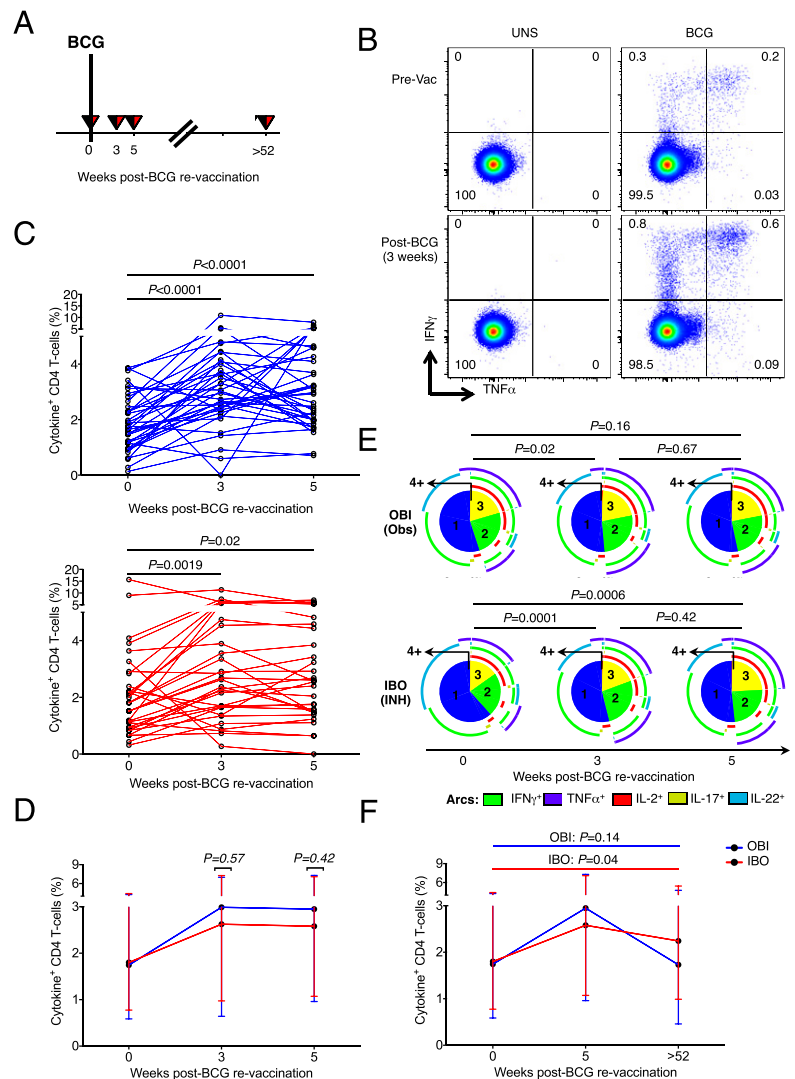
blood count, hemoglobin levels, QuantiFERON positivity rate, or size of TST induration. IPT adherence during the trial was excellent for both study arms; 87% of all urine INH metabolite tests performed during the trial were positive (18).

### Minor effect of IPT on total mycobacteria-specific immune responses

We first sought to determine whether preclearance of underlying *M. tuberculosis* infection with INH modulates cytokine coexpression patterns and/or frequencies of *M. tuberculosis*-specific T cells. Total ESAT-6/CFP-10-specific CD4 and CD8 responses, defined as cells expressing any of the five cytokines, decreased after enrollment in both groups (IBO,  $p = 0.0076$ ; OBI,  $p = 0.0005$ ). This decline was not different between participants who received IPT and those who did not (Fig. 2A) and, therefore, suggests that IPT did not modulate frequencies of mycobacteria-specific CD4 T cells. Frequencies of ESAT-6/CFP-10-specific CD8 responses were too low to accurately define cytokine coexpression patterns (Fig. 2A). IFN- $\gamma$ , TNF- $\alpha$ , IL-2, IL-17, and/or IL-22 coexpression profiles of ESAT-6/CFP-10-specific CD4 T cells were not modulated by IPT (Fig. 2B). Similarly, no differences were observed in  $\gamma\delta$  T cell, CD3<sup>+</sup>CD56<sup>+</sup> NKT-like cell, or CD3<sup>+</sup>CD56<sup>dim</sup> or CD3<sup>+</sup>CD56<sup>hi</sup> NK cell responses to ESAT-6/CFP-10 stimulation between the two groups (Supplemental Fig. 2A).

We also analyzed effects of IPT on frequencies of BCG-reactive CD4, CD8, and  $\gamma\delta$  T cells, CD3<sup>+</sup>CD56<sup>+</sup> NKT-like cells, and

**FIGURE 3.** BCG-specific CD4 T cell responses after BCG revaccination. **(A)** Schematic diagram of blood draws to assess BCG-specific T cell responses after revaccination. **(B)** Representative flow cytometry plots of CD4 T cells in one OBI participant. TNF- $\alpha$  versus IFN- $\gamma$  profiles before BCG vaccination (upper panels) and 3 wk postvaccination (lower panels) in the unstimulated (UNS; left panels) or BCG-stimulated (right panels) samples. **(C)** Total frequencies of BCG-specific cytokine-positive CD4 T cells in all participants from the OBI group (upper panel) or the IBO group (lower panel). The  $p$  values were calculated using the Wilcoxon signed-rank test, comparing the pre- and postvaccination visits. Bonferroni-adjusted  $p$  value threshold of 0.025 after correcting for the two performed comparisons was considered statistically significant. **(D)** Median (error bars represent interquartile range [IQR]) frequencies of BCG-induced CD4 T cell responses. Blue and red lines correspond to the group pretreated (IBO) or not treated (OBI) with INH for 6 mo, respectively. Unadjusted  $p$  values were calculated using the Mann–Whitney  $U$  test, comparing the two groups. **(E)** Median proportions of BCG-specific CD4 T cells coexpressing IFN- $\gamma$ , TNF- $\alpha$ , IL-2, IL-17, and/or IL-22 in groups observed only (OBI; upper panel) or pretreated with INH for 6 mo (IBO; lower panel). Numbers in the pie slices indicate the number of coexpressed cytokines. Arcs represent the cytokines expressed within each pie slice. The  $p$  values were calculated using a nonparametric paired permutation test comparing the proportions of subsets between two pies. **(F)** Median (error bars denote IQR) frequencies of BCG-specific cytokine responses 1 y postvaccination to pre-BCG baseline: total expression of at least one of five cytokines (IL-2, IL-17, IL-22, IFN- $\gamma$  and TNF- $\alpha$ ) in CD4 T cells. The  $p$  values were calculated using the Wilcoxon signed-rank test between baseline and 1-y postvaccination responses within each group. Bonferroni adjusted  $p$  value threshold of 0.025 was considered statistically significant.



CD3<sup>-</sup>CD56<sup>+</sup> NK cells and observed no marked differences (Fig. 2C, Supplemental Fig. 2B). However, in the IPT-treated group, the relative proportions of IL-22-expressing cells among total cytokine-expressing BCG-specific CD4 T cells increased, whereas the proportions of cells expressing IFN- $\gamma$  decreased. This was not observed in the group not treated with IPT (Fig. 2D).

#### BCG transiently boosted mycobacteria-specific CD4, CD8, and $\gamma\delta$ T cell responses

We also determined whether BCG revaccination boosted mycobacteria-specific CD4 T cell responses in adults who were highly sensitized to mycobacterial Ags (Fig. 3A). Relative to the prevaccination time point, we observed increased frequencies of total cytokine-expressing BCG-specific CD4 responses at 3 and 5 wk after BCG revaccination (Fig. 3B, 3C). This finding was observed irrespective of whether participants received IPT pretreatment (Fig. 3C, 3D). However, BCG revaccination resulted in a decrease in proportions of IL-22-expressing BCG-specific CD4 T cells in the INH-pretreated group only (Fig. 3E). In both groups, total BCG-specific responses reverted to baseline levels 1 y after revaccination (Fig. 3F).

Similarly to CD4 T cells, frequencies of IFN- $\gamma$ -expressing CD8 and  $\gamma\delta$  T cells were transiently boosted by BCG revaccination, although to a lesser magnitude (Fig. 4). BCG-reactive CD8 T,  $\gamma\delta$  T, CD3<sup>+</sup>CD56<sup>+</sup> NKT-like, and CD56<sup>dim</sup> and CD56<sup>hi</sup> NK cells predominantly expressed IFN- $\gamma$  (Supplemental Fig. 3A). Therefore, we analyzed frequencies of total BCG-reactive IFN- $\gamma$ -expressing cells to simplify the analysis. At 1 y postvaccination, BCG-specific IFN- $\gamma$ -expressing CD8 and  $\gamma\delta$  T cells had reverted to levels observed before BCG revaccination, irrespective of IPT pretreatment (Fig. 4C, 4F).

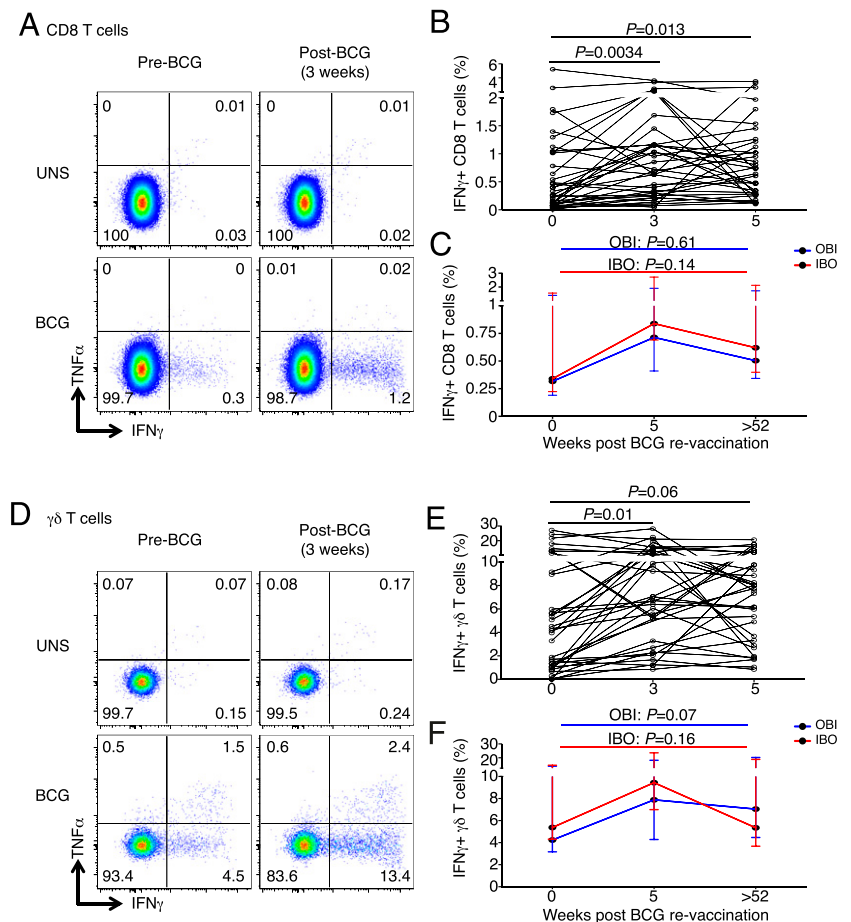
#### BCG revaccination induces durable CD3<sup>+</sup>CD56<sup>+</sup> NKT-like cell responses

*M. tuberculosis*-specific CD3<sup>+</sup>TCRV $\beta$ 11<sup>+</sup> NKT cells were recently shown to contribute to the antimycobacterial immune response (21). We also sought to determine whether BCG revaccination boosted BCG-reactive CD3<sup>+</sup>CD56<sup>+</sup> NKT-like cell responses. Before vaccination, IPT preclearance had no effect on frequencies of BCG-reactive CD3<sup>+</sup>CD56<sup>+</sup> NKT-like cells (Supplemental Fig. 2B). Frequencies of BCG-reactive IFN- $\gamma$ -expressing CD3<sup>+</sup>CD56<sup>+</sup> NKT-like cells significantly increased above baseline levels 3 and 5 wk after BCG revaccination (Fig. 5A, 5B). Remarkably, however, these BCG-reactive CD3<sup>+</sup>CD56<sup>+</sup> NKT-like cell responses remained above baseline levels up to 1 y postvaccination in the IBO group (Fig. 5C), suggesting that BCG revaccination boosted highly durable NKT-like cell responses.

#### BCG revaccination induces highly durable CD56<sup>dim</sup> and CD56<sup>hi</sup> NK cell responses

A recent study (22) reported no changes in IFN- $\gamma$ -expressing NK cell frequencies after BCG vaccination in humans but showed that BCG-induced heterologous protective immunity against disseminated *Candida albicans* infection in SCID mice was partially dependent on NK cells. To determine whether BCG revaccination of persons with underlying LTBI boosted mycobacteria-reactive NK cell responses, we quantified cytokine-expressing CD56<sup>dim</sup> and CD56<sup>hi</sup> NK cells (Fig. 5D, 5G). BCG-reactive CD56<sup>dim</sup> and CD56<sup>hi</sup> NK cells expressed almost exclusively IFN- $\gamma$  and none of the other four cytokines (Supplemental Fig. 3A). Surprisingly, frequencies of IFN- $\gamma$ -expressing CD56<sup>dim</sup> and CD56<sup>hi</sup> NK cells rapidly increased by 3 wk in both groups and remained significantly

**FIGURE 4.** Cytokine-expression by BCG-reactive cell subsets before and after BCG revaccination. **(A)** Representative plots showing BCG-reactive IFN- $\gamma$  and TNF- $\alpha$  expression by CD8 T cells before BCG vaccination (pre-BCG vaccination; left panels) and 3 wk postvaccination (right panels) in unstimulated (UNS; upper panels) or BCG-stimulated (BCG; lower panels) samples. **(B)** BCG-specific IFN- $\gamma$  expression by CD8 T cells 3–5 wk postvaccination in the OBI group. Each line represents an individual. The *p* values were calculated using the Wilcoxon signed-rank test between baseline and 3 or 5 wk postvaccination. Bonferroni adjusted *p* value threshold of 0.025 was used to correct for the two comparisons. **(C)** Median (error bars denote interquartile) responses in the IBO (red) or OBI (blue) groups 1 y after BCG revaccination. **(D–F)** BCG-reactive cytokine expression by  $\gamma\delta$  T cells, shown in identical graphs as those for CD8 T cells.



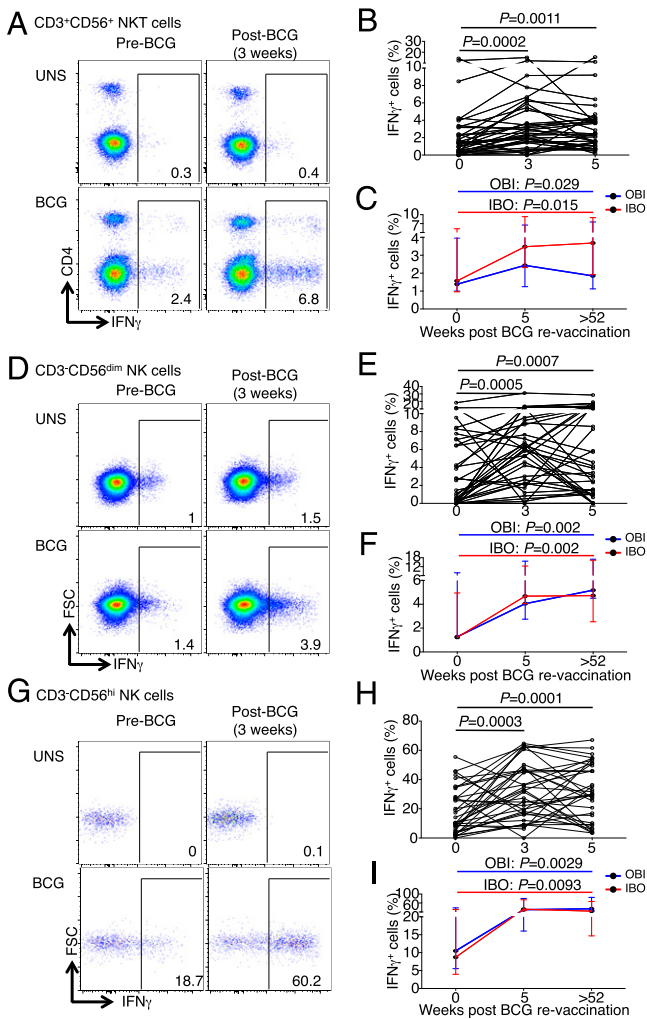


**FIGURE 5.** Frequencies of cytokine-expressing BCG-reactive CD3<sup>+</sup>CD56<sup>+</sup> NKT-like, CD3<sup>+</sup>CD56<sup>dim</sup> NK, and CD3<sup>+</sup>CD56<sup>hi</sup> NK cells after BCG revaccination. **(A)** Representative flow cytometry plots depicting IFN- $\gamma$ -expressing cells in BCG-reactive CD3<sup>+</sup>CD56<sup>+</sup> NKT-like cells. **(B)** Frequencies of BCG-reactive IFN- $\gamma$ -expressing cells within each cell subset in participants from the OBI group only. Unadjusted *p* values, calculated using the Wilcoxon signed-rank test, represent comparisons between time points. **(C)** Comparison of median (error bars denote interquartile) BCG-specific IFN- $\gamma$  responses 1 y postvaccination with pre-BCG baseline. The *p* values were calculated, using the Wilcoxon signed-rank test, comparing responses at baseline and 1 y postvaccination. Bonferroni-adjusted *p* value threshold of 0.025 was used to correct for the two performed comparisons in **(B)** and **(C)**. Similar graphs are shown for CD3<sup>+</sup>CD56<sup>dim</sup> NK cells **(D–F)** and CD3<sup>+</sup>CD56<sup>hi</sup> NK cells **(G–I)**.

above baseline 5 wk after BCG revaccination (Fig. 5E, 5H), irrespective of pretreatment with INH (Supplemental Fig. 3B). Longer follow-up revealed that these BCG-reactive NK cell responses were even more durable, with little to no sign of waning. By 1 y after BCG revaccination, frequencies of IFN- $\gamma$ -expressing BCG-reactive CD56<sup>dim</sup> and CD56<sup>hi</sup> NK cells were markedly higher than those observed before BCG revaccination (Fig. 5F, 5I).

#### *BCG-responsive IFN- $\gamma$ -expressing CD56<sup>dim</sup> and CD56<sup>hi</sup> NK cells are distinct NK cell subsets with effector function*

The highly durable BCG-reactive NK cell responses prompted us to explore phenotypic and/or functional markers that may associate with their memory characteristics. We measured cell surface expression of CD57, CD158b, CD161, CD8, and CD16 (Fc $\gamma$ RIII), as well as intracellular expression of IFN- $\gamma$  and perforin, by CD56<sup>dim</sup>

and CD56<sup>hi</sup> NK cells in a subset of 19 participants from the IBO group (Supplemental Table I). Within the entire NK cell population, CD16 was expressed highly on CD56<sup>dim</sup>, but not CD56<sup>hi</sup>, NK cells, as previously described (23). As a consequence, we included CD16 as an additional lineage marker to differentiate CD56<sup>dim</sup> and CD56<sup>hi</sup> NK cells in subsequent analyses (Fig. 6A). Expression of the NK cell surface markers CD57, CD158b, CD161, and CD8 was more heterogeneous in bulk CD56<sup>dim</sup>CD16<sup>+</sup> NK cells than in CD56<sup>hi</sup>CD16<sup>lo</sup> NK cells (Fig. 6B, 6C). Although both NK cell subsets expressed perforin, the CD56<sup>dim</sup>CD16<sup>+</sup> NK cell subset expressed higher levels (Fig. 6A, 6D). This is consistent with the previously reported greater cytotoxic potential of the CD56<sup>dim</sup>CD16<sup>+</sup> NK cell subset (23). Relative to unstimulated samples, BCG stimulation also induced higher expression of perforin in CD56<sup>hi</sup>CD16<sup>lo</sup>, but not CD56<sup>dim</sup>CD16<sup>+</sup>, NK cells (Fig. 6E). At 1 y after BCG revaccination, BCG-stimulated CD56<sup>hi</sup>CD16<sup>lo</sup> NK cells expressed higher levels of perforin compared with baseline (unadjusted *p* = 0.023), suggesting a highly durable BCG-mediated modulation of cytotoxic effector function.

One explanation for the memory function of NK cells may be that BCG induces NK cell differentiation, as reported previously (22). To explore this, we compared the immunophenotypes of NK cells before and after BCG revaccination. No marked changes in cell surface expression of CD57, CD158b, CD161, or CD8 were detected for either NK cell subset following BCG revaccination (Fig. 6C). The predominant BCG-reactive, IFN- $\gamma$ -expressing CD56<sup>hi</sup>CD16<sup>lo</sup> and CD56<sup>dim</sup>CD16<sup>+</sup> NK cell subsets expressed a CD8<sup>−</sup>CD57<sup>−</sup>CD158b<sup>−</sup>CD161<sup>+</sup> phenotype (Fig. 6C).

The unexpected responses by these lymphocyte subsets to BCG revaccination prompted us to explore their relative contributions to the IFN- $\gamma$  response to BCG. Although  $\gamma\delta$  T cells, NKT-like cells, and CD56<sup>dim</sup> and CD56<sup>hi</sup> NK cells constitute less than a quarter of the lymphocytes in peripheral blood, these cells collectively account for approximately half of the overall BCG-specific IFN- $\gamma$ -expressing cellular response (Fig. 6F).

#### *BCG-responsive IFN- $\gamma$ -expressing NKT-like and NK cells are induced by BCG vaccination in infants*

Viral infections, such as CMV, were reported to sensitize NK cells to differentiate into adaptive “memory” NK cells with enhanced antiviral responses (24, 25). Based on our observed enhanced NK cell responses to BCG following revaccination (Fig. 5D–H), we hypothesized that BCG vaccination of mycobacteria-naïve infants would sensitize BCG-reactive memory NK cell responses. Consequently, we measured frequencies of IFN- $\gamma$ -expressing BCG-reactive CD56<sup>dim</sup>CD16<sup>+</sup> and CD56<sup>hi</sup>CD16<sup>lo</sup> cells in 5-wk-old infants who did or did not receive BCG at birth (Fig. 7). Frequencies of IFN- $\gamma$ -expressing BCG-reactive CD56<sup>dim</sup>CD16<sup>+</sup> and CD56<sup>hi</sup>CD16<sup>lo</sup> cells were very low in unvaccinated infants (Fig. 7B, 7C). By contrast, infants who received routine BCG vaccination at birth had high levels of IFN- $\gamma$ -expressing NK cells (Fig. 7B, 7C). Interestingly, BCG vaccination also induced high frequencies of IFN- $\gamma$ -expressing BCG-reactive CD3<sup>+</sup>CD56<sup>+</sup> NKT-like cells (Fig. 7B, 7C).

#### *BCG-responsive IFN- $\gamma$ -expressing NKT-like and NK cells are activated by IL-12 and IL-18*

A possible mechanism underlying the highly durable BCG-induced NK cell memory response is through bystander activation by cytokines expressed by conventional BCG-specific memory T cells. Two studies (26, 27) reported that durable NK cell responses induced by rabies virus vaccination, or a novel TB vaccine candidate, were associated with IL-2 expressed by Ag-specific CD4



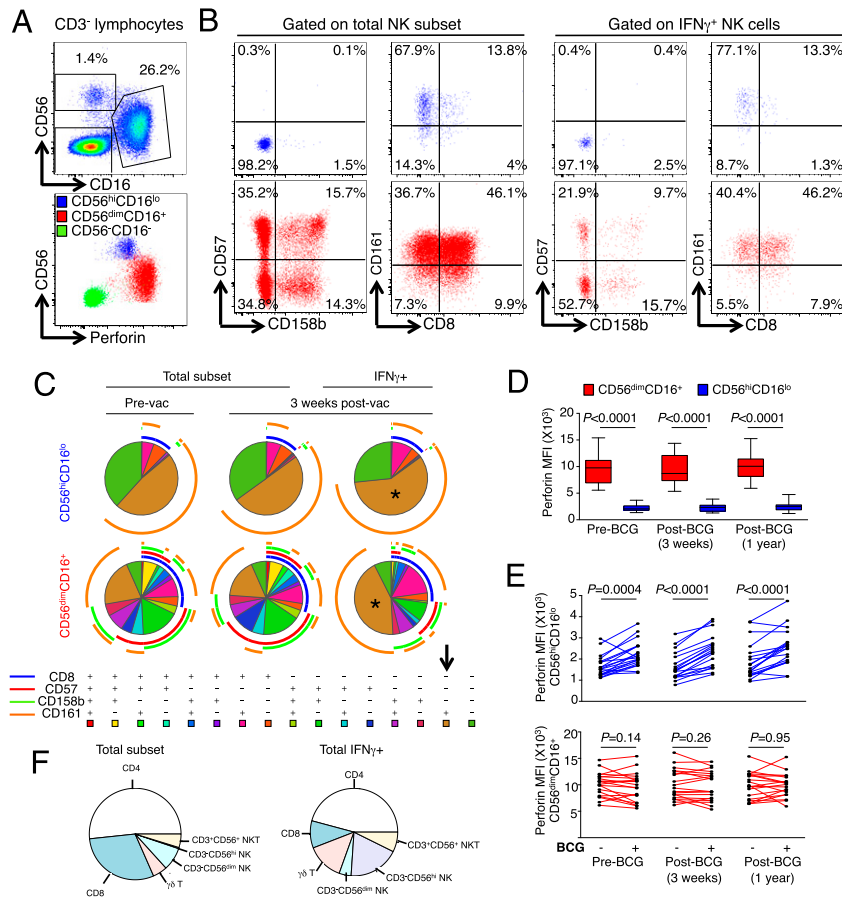


**FIGURE 6.** Functional and phenotypic characterization of BCG-reactive CD56<sup>dim</sup> and CD56<sup>hi</sup> NK cells. **(A)** Representative flow cytometry plots of CD16 and CD56 expression by CD3<sup>+</sup> lymphocytes to identify NK cell subsets: CD56<sup>hi</sup>CD16<sup>lo</sup> and CD56<sup>dim</sup>CD16<sup>+</sup> populations (upper panel). Perforin expression by NK cell subsets and CD3<sup>+</sup>CD56<sup>−</sup>CD16<sup>−</sup> non-T or NK cells plotted against CD56 expression (lower panel). **(B)** Representative plots of total (left panels) CD56<sup>hi</sup>CD16<sup>−</sup> cells (blue plots; upper panels) and CD56<sup>dim</sup>CD16<sup>+</sup> cells (red plots; lower panels) and BCG-reactive IFN- $\gamma$ -expressing cells (right panels) showing coexpression patterns of CD158b/CD57 (left panels) and CD8/CD161 (right panels). **(C)** Combinatorial expression of CD8, CD57, CD158b, and CD161 as median proportions of CD56<sup>hi</sup>CD16<sup>lo</sup> cells (upper panels) and CD56<sup>dim</sup>CD16<sup>+</sup> cells (lower panels) in total NK cell populations before vaccination (left panels) or 3 wk post-BCG revaccination (middle panels) or only within BCG-reactive IFN- $\gamma$ -expressing NK cells 3 wk post-revaccination (right panels). Asterisks and arrow correspond to the predominant CD8<sup>−</sup>CD57<sup>−</sup>CD158b<sup>−</sup>CD161<sup>+</sup> Boolean combination in both NK subsets. **(D)** Box-and-whisker plots of perforin median fluorescence intensities (MFI) in BCG-stimulated CD56<sup>hi</sup>CD16<sup>−</sup> and CD56<sup>dim</sup>CD16<sup>+</sup> NK cells. Horizontal lines represent medians, the boxes represent the interquartile range, and the whiskers represent the range. Unadjusted *p* values were calculated with the Wilcoxon signed-rank test between the two subsets at vaccination baseline (pre-BCG) and at 3 wk and 1 y postrevaccination. **(E)** Perforin expression, measured as MFI, in a paired analysis of unstimulated and BCG-stimulated samples in CD56<sup>hi</sup>CD16<sup>−</sup> cells (upper panel) and CD56<sup>dim</sup>CD16<sup>+</sup> cells (lower panel). Unadjusted *p*-values were calculated with the Wilcoxon signed-rank test. **(F)** Median proportions of the respective lymphocyte subsets within peripheral blood 3 wk postvaccination in the IBO group (left panel) or the median proportional contribution of these lymphocyte subsets to the total BCG-reactive IFN- $\gamma$ <sup>+</sup> cells (right panel).

T cells. Therefore, we investigated associations between frequencies of BCG-reactive NK cell memory responses and cytokine-expressing BCG-specific CD4 T cells in the adults who received BCG revaccination. We detected a moderate positive correlation between frequencies of BCG-specific IL-2-expressing CD4 T cells and BCG-reactive IFN- $\gamma$ -expressing CD56<sup>hi</sup>CD16<sup>lo</sup> and CD56<sup>dim</sup>CD16<sup>+</sup> NK cells 3 wk following revaccination (Fig. 8A). However, this association was not observed before or 1 y after BCG revaccination (Fig. 8A). Because BCG-specific IL-2-expressing memory CD4 T cells were not maintained for 52 wk (Figs. 3, 8B), this bystander activation may only partially explain the NK cell memory response. Furthermore, although PHA stimulation induced high frequencies of IL-2-expressing CD4 T cells, this was not associated with enhanced IFN- $\gamma$ -expressing memory NK cells as seen with BCG stimulation (Fig. 8B).

Therefore, we sought to determine to what degree IFN- $\gamma$  expression by NK cells after BCG stimulation was dependent on IL-2, or the proinflammatory innate cytokines IL-12 and IL-18, which

were reported to promote NK cell responses (28, 29). Stimulation of whole blood with rIL-2 alone induced IFN- $\gamma$  expression from a moderate proportion of CD56<sup>dim</sup>CD16<sup>+</sup> and CD56<sup>hi</sup>CD16<sup>lo</sup> NK cells (Fig. 8C, 8D). Stimulation with rIL-12 and rIL-18 in the absence of BCG markedly enhanced the proportion of responding NK cells.

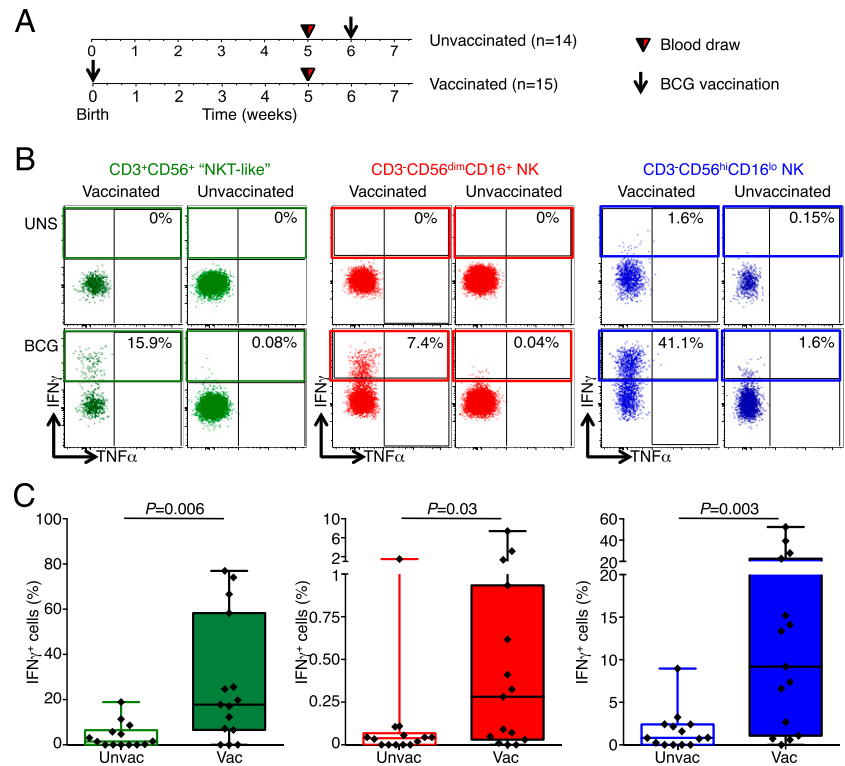
Conversely, blocking IL-12 and IL-18 with neutralizing Abs nearly completely abolished BCG-induced IFN- $\gamma$  expression by CD56<sup>dim</sup>CD16<sup>+</sup> and CD56<sup>hi</sup>CD16<sup>lo</sup> NK cells (Fig. 8E). Blocking with IL-2 alone did not significantly reduce the NK cell response to BCG (Fig. 8E). Collectively, these data suggest that BCG-induced IFN- $\gamma$  expression by NK cells is entirely dependent on bystander stimulation with the innate cytokines IL-12 and IL-18.

## Discussion

In this study, we addressed three critical immunological questions related to TB-prevention strategies in endemic areas (30): whether INH treatment of *M. tuberculosis*-sensitized adults modulated



**FIGURE 7.** IFN- $\gamma$ -expressing BCG-reactive CD3<sup>+</sup>CD56<sup>+</sup> NKT-like, CD3<sup>-</sup>CD56<sup>dim</sup> NK, and CD3<sup>-</sup>CD56<sup>hi</sup> NK cells are induced by BCG vaccination. **(A)** Design of delayed-BCG vaccination study in infants. Schematic representation of vaccination and blood draws for BCG-unvaccinated (delayed) and BCG-vaccinated infants. Blood was drawn at 5 wk of age in both groups. **(B)** Representative flow cytometry plots depicting TNF- $\alpha$  versus IFN- $\gamma$  expression in CD3<sup>+</sup>CD56<sup>+</sup> NKT-like cells (left panels), CD3<sup>-</sup>CD56<sup>dim</sup>CD16<sup>+</sup> NK cells (middle panels), and CD3<sup>-</sup>CD56<sup>hi</sup>CD16<sup>lo</sup> NK cells (right panels) in unstimulated (upper panels) or BCG-stimulated (lower panels) samples from a vaccinated (left panels) or unvaccinated (right panels) infant. **(C)** Frequencies of BCG-reactive IFN- $\gamma$ <sup>+</sup> CD3<sup>+</sup>CD56<sup>+</sup> NKT-like cells (left panel), CD3<sup>-</sup>CD56<sup>dim</sup>CD16<sup>+</sup> NK cells (middle panel), and CD3<sup>-</sup>CD56<sup>hi</sup>CD16<sup>lo</sup> NK cells (right panel). Horizontal lines represent medians, boxes represent the interquartile range, and whiskers represent the range. Unadjusted *p* values were calculated with the Mann–Whitney *U* test, comparing frequencies of cytokine-positive cells between the two groups. The *p* values < 0.05 were considered statistically significant.



mycobacteria-specific immune responses; whether BCG revaccination boosted pre-existing mycobacteria-specific responses in adults with previous exposure and sensitization to *M. tuberculosis*; and whether BCG revaccination induced durable changes to BCG-reactive lymphocytes.

Our data showed that IPT had little detectable impact on the magnitude or cytokine-expression profiles of conventional mycobacteria-specific T cells or BCG-reactive CD3<sup>+</sup>CD56<sup>+</sup> NKT-like and CD3<sup>-</sup>CD56<sup>+</sup> NK cell responses in peripheral blood. This was consistent with previous studies (11–16) that measured effects of IPT on frequencies of Ag-specific T cells, although other studies (8–10) reported decreases in Ag-specific T cell responses after IPT. One exception was an unexpected moderate proportional increase in frequencies of BCG-specific IL-22-expressing CD4 T cells, which was reversed following BCG revaccination. Higher levels of IL-22 were reported in the bronchoalveolar lavage fluid of pulmonary TB patients relative to healthy individuals (31), suggesting a role for IL-22 in the immune response to *M. tuberculosis*. Thus, it remains possible that higher proportions of BCG-specific IL-22-expressing CD4 T cells in peripheral blood are associated with IPT-induced reduction in Ag load at the infection site. Revaccination with BCG reversed the relative proportions of IL-22 and IFN- $\gamma$ , potentially through reintroduction of Ag at the injection site (Fig. 3E).

A moderate decrease in ESAT-6/CFP-10-specific CD4 T cell responses was observed in both groups, independently of IPT treatment. This was consistent with the previously reported decrease in *M. tuberculosis*-specific IFN- $\gamma$  responses measured by QuantiFERON TB-Gold In-Tube assay in these groups (17) and is likely the result of waning T cell responses following a transient boost by TST, performed at screening (32). Detection of cytokine-expressing NK and  $\gamma\delta$  T cell responses after ESAT-6/CFP-10 stimulation was likely a result of bystander activation from Ag-specific cytokine-expressing ESAT-6/CFP-10-specific CD4 and/or CD8 T cells. Collectively, we found no evidence to suggest that INH preclearance of *M. tuberculosis* might compromise the

durability of mycobacteria-specific immune responses (8), at least in the short-term. However, given the high levels of *M. tuberculosis* transmission in the study setting in South Africa (32), it is possible that some participants may have been re-exposed and/or reinfected, which may, in turn, boost levels of mycobacteria-specific memory T cells.

We reported previously that BCG revaccination of these *M. tuberculosis*-sensitized, TST-positive adults appeared safe and well tolerated (18). We now demonstrate that BCG revaccination transiently boosted Th1 cytokine-expressing, mycobacteria-specific CD4, CD8, and  $\gamma\delta$  T cell responses despite high levels of prior *M. tuberculosis* sensitization. IPT pretreatment also did not affect BCG boosting of these responses. The transient nature of these T cell responses was not surprising given the high baseline magnitude of *M. tuberculosis*-specific T cell responses. This may represent an example of masking of the BCG-induced immune response, which was described previously in children (33). Nevertheless, we demonstrate that BCG is immunogenic, even in the context of prior sensitization, providing evidence against the contrary hypothesis of immunological blocking of the BCG-induced immune response (34). Our study does not address whether these findings have implications for BCG-induced protective immunity. Frequencies and cytokine-expression profiles of BCG-specific CD4, CD8, and  $\gamma\delta$  T cells did not correlate with risk for TB in 10-wk-old infants (35), highlighting the importance of broadening our assessment of BCG-reactive immune responses.

To our knowledge, we show for the first time in humans that TB vaccine-boosted CD3<sup>+</sup>CD56<sup>+</sup> NKT-like cell responses persisted for up to 1 y postvaccination, suggesting memory function akin to conventional T cells. This is consistent with a recent report (36) that BCG vaccination of nonhuman primates induced IFN- $\gamma$ -expressing glucose monomycolate-specific NKT cell responses. Mycolic acids, including glucose monomycolates, are present on *M. tuberculosis* and BCG and are recognized by CD1b-restricted (37) and CD1c-restricted (36) NKT cells. Interestingly, CD1c-restricted NKT cell responses were reported to be inhibited by

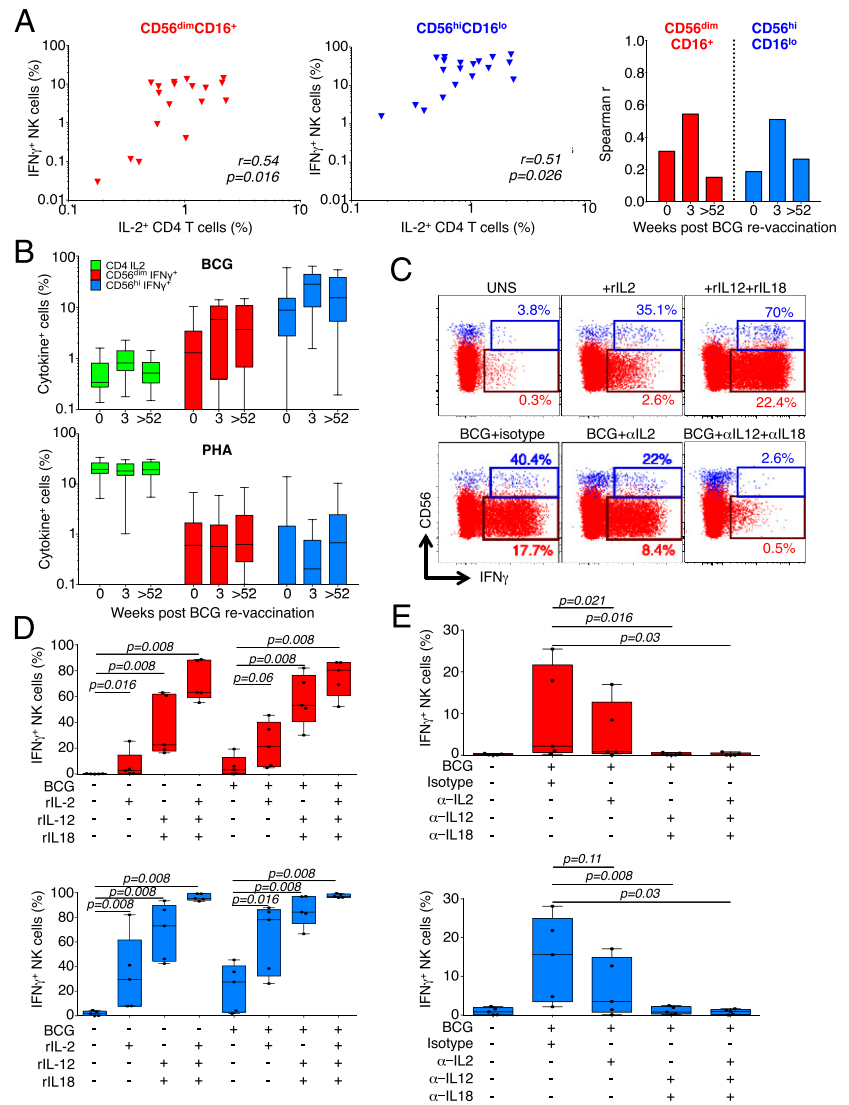


**FIGURE 8.** Bystander activation of BCG-reactive NK cell IFN- $\gamma$  expression. **(A)** Frequencies of BCG-specific IL-2-expressing CD4<sup>+</sup> T cells and IFN- $\gamma$ -expressing CD56<sup>dim</sup>CD16<sup>+</sup> (left panel) or CD56<sup>hi</sup>CD16<sup>-</sup> (middle panel) NK cells at 3 wk post-BCG revaccination in the BCG-revaccination trial. Unadjusted *p* values and correlation coefficients were calculated with the Spearman's nonparametric correlation test. Spearman's *r* coefficients before BCG vaccination and at 3 wk or 1 y following BCG revaccination (right panel). **(B)** Frequencies of IL-2-expressing CD4<sup>+</sup> T cells (green), IFN- $\gamma$ -expressing CD3<sup>-</sup>CD56<sup>dim</sup>CD16<sup>+</sup> NK cells (red), and CD3<sup>-</sup>CD56<sup>hi</sup>CD16<sup>lo</sup> NK cells (blue) in samples stimulated with BCG (upper panel) or PHA (lower pattern). Horizontal lines represent medians, boxes represent the interquartile range, and whiskers represent the range. **(C)** Representative flow cytometry plots of IFN- $\gamma$  expression in CD3<sup>-</sup>CD56<sup>dim</sup>CD16<sup>+</sup> NK cells (red) and CD3<sup>-</sup>CD56<sup>hi</sup>CD16<sup>lo</sup> NK cells (blue) in whole blood from healthy donors incubated with the indicated cytokines, blocking Abs, or BCG. **(D and E)** Frequencies of IFN- $\gamma$ -expressing CD3<sup>-</sup>CD56<sup>dim</sup>CD16<sup>+</sup> NK cells (upper panel) and CD3<sup>-</sup>CD56<sup>hi</sup>CD16<sup>lo</sup> NK cells (lower panel) in blood from five donors incubated with the indicated cytokines, blocking Abs, and/or BCG. Unadjusted *p* values were calculated with the Wilcoxon signed-rank test.

INH therapy (38). We cannot rule out that the CD1-restricted NKT cell subset was modulated by IPT in our study. Because we used CD3<sup>+</sup>CD56<sup>+</sup> as a broad heterogeneous definition of NKT cells, we were not able to definitively identify CD1-restricted NKT cells. Ongoing work aims to elucidate the memory potential of specific CD1-restricted T cells in response to BCG, as a model for whole-cell TB vaccines, using CD1 tetramers (39).

The most intriguing finding in this study is that BCG revaccination boosted peripheral blood BCG-reactive CD56<sup>hi</sup>CD16<sup>lo</sup> and CD56<sup>dim</sup>CD16<sup>+</sup> NK cells, which persisted for a very long time,  $\geq 1$  y after vaccination. The dependence of IFN- $\gamma$ -expressing NK cell responses on prior BCG vaccination in infants is consistent with adaptation of these NK cells to display immunological memory. Such innate cell memory function was attributed to epigenetic modifications in previous studies. For example, CMV was shown to induce durable genome-wide epigenetic footprints in signaling adaptors of NK cells, such as SYK (40). These epigenetic changes modulated Ab-dependent expansion of CMV-reactive NK cells through reduced Fc $\gamma$ R expression (41). Epigenetic modification of NK cells was also suggested to underlie BCG-induced cross-protection against related pathogens, such as *Mycobacterium leprae* (42), and *C. albicans* (22). Our phenotypic profiling of CD56<sup>dim</sup> and CD56<sup>hi</sup> NK cells, based on a limited set of NK markers, did not support striking differentiation of BCG-reactive NK cells. However, in infants not exposed to mycobacteria,

BCG-reactive IFN- $\gamma$ -expressing CD56<sup>hi</sup> NK cells were expanded in vaccinated infants (Fig. 7). Therefore, BCG may induce epigenetic modifications and differentiation of NK cells, but we only tested a limited repertoire of NK cell receptors as a surrogate for differentiation. Alternatively, BCG was shown to induce immune training via NOD2-mediated epigenetic modification of monocyte inflammatory genes (43). Such epigenetic modifications of monocytes could result in enhanced IL-12 and IL-18 production to indirectly drive sustained NK cell activation upon restimulation (44). Finally, BCG vaccination also expands the frequencies of BCG-specific IL-2<sup>+</sup> conventional CD4 T cells (45), which may indirectly expand BCG-reactive NK cells. Our study design did not allow identification of the exact mechanism underlying the BCG-induced memory response by NK cells.

A previous study (46) reported BCG-induced unconventional CD4<sup>-</sup>CD8<sup>-</sup> T cells, including  $\gamma\delta$  T cells and possibly NK cells, in 10-wk-old infants with no prior mycobacterial sensitization who had received BCG at birth. Because BCG-induced conventional CD4 and CD8 T cell responses peak at 10 wk of age (47), it is possible that BCG-reactive recall responses by unconventional cells were indirectly activated by cytokines expressed by BCG-specific conventional T cells. NK cell recall responses were shown to depend on IL-2 expressed by Ag-specific CD4 T cells, as well as IL-12 and IL-18 from other accessory cells. In the current study, frequencies of IL-2-expressing BCG-specific CD4 responses

correlated weakly with IFN- $\gamma$ -expressing BCG-reactive NK cells. However, induction of IL-2 by PHA stimulation or addition of rhIL-2, as well as the more durable BCG-reactive NK cell responses observed post-BCG revaccination, suggests that IL-2 was not the primary driver of BCG-reactive NK responses. In fact, no clear sign of waning of these memory NK cell populations was detected even 1 y after BCG revaccination. It was clear, nonetheless, that IL-12 and IL-18 were indispensable for IFN- $\gamma$  production by CD56<sup>hi</sup>CD16<sup>lo</sup> and CD56<sup>dim</sup>CD16<sup>+</sup> BCG-reactive NK cells. IL-12 signaling was shown to be required for the generation and maintenance of CMV-reactive memory NK cells (29). Furthermore, IL-18 signaling downstream of *M. tuberculosis* infection in mice was recently shown to be critical for IFN- $\gamma$  production by NK cells, which conferred partial protection independently of Ag-specific T cell responses (28).

Interestingly, we found that CD56<sup>dim</sup> and CD56<sup>hi</sup> NK cell subsets contributed differentially to the BCG-specific response. Perforin expression was universally high in CD56<sup>dim</sup> cells, whereas its expression was inducible in CD56<sup>hi</sup> cells by BCG stimulation. We show that BCG-responsive IFN- $\gamma$ -expressing NK cells predominantly expressed CD161 but not CD158b or CD57. CD161 expression was associated with activation in immature NK cells (48), whereas expression of NK cell receptor CD158b (KIR2DL2/DL3) (49) and CD57 (50) on CD56<sup>+</sup> NK cells was associated with attenuation of NK cell functions in chronic infections. Therefore, our data suggest that BCG-boosted NK cells are in an early or intermediate stage of differentiation. Under this hypothesis, high mycobacterial loads, for instance during active TB disease, may drive NK cell differentiation toward a more differentiated CD158b<sup>+</sup>CD57<sup>+</sup> phenotype with possible compromise of IFN- $\gamma$  expression, as previously shown in response to viral infections (49, 50). Regardless, we did not observe any changes in NK cell phenotype after BCG revaccination that may be associated with the observed memory characteristic.

In conclusion, our study demonstrates the impact of BCG revaccination on properties of mycobacteria-induced responses in *M. tuberculosis*-sensitized populations. NKT-like and NK cell memory responses may be novel targets for induction by new TB vaccines in endemic countries. Further work is needed to investigate how new vaccines modulate NK cell functions and whether these NK cells may contribute to protective immunity to TB. Systematic testing and treatment of LTBI is recommended for persons at risk for progressing to active disease in high-income or upper middle-income countries with estimated TB incidence rates < 100/100,000 population (51). In resource-limited and middle-income countries with TB incidence rates > 100/100,000 population, IPT for treatment of LTBI is recommended only for children <5 y of age and people living with HIV (51). Because INH preclearance of latent *M. tuberculosis* bacilli had no marked effect on the magnitude, persistence, or functional attributes of lymphocyte responses boosted by BCG, prevaccination IPT would likely neither interfere with nor enhance the protective efficacy of new TB vaccines and vaccination strategies.

## Disclosures

The authors have no financial conflicts of interest.

## References

- Eurosurveillance Editorial Team. 2013. WHO publishes global tuberculosis report 2013. *Euro. Surveill.* 18. Available at: <http://www.eurosurveillance.org/images/dynamic/EE/N18N43/art20615.pdf>.
- Dye, C., S. Scheele, P. Dolin, V. Pathania, and M. C. Ravigliione. 1999. Consensus statement. Global burden of tuberculosis: estimated incidence, prevalence, and mortality by country. WHO Global Surveillance and Monitoring Project. *JAMA* 282: 677–686.
- Smieja, M. J., C. A. Marchetti, D. J. Cook, and F. M. Smail. 2000. Isoniazid for preventing tuberculosis in non-HIV infected persons. *Cochrane Database Syst. Rev.* (2): CD001363.
- Churchyard, G. J., K. L. Fielding, J. J. Lewis, L. Coetzee, E. L. Corbett, P. Godfrey-Faussett, R. J. Hayes, R. E. Chaisson, and A. D. Grant, Thibela TB Study Team. 2014. A trial of mass isoniazid preventive therapy for tuberculosis control. *N. Engl. J. Med.* 370: 301–310.
- Wood, R., and L. G. Bekker. 2014. Isoniazid preventive therapy for tuberculosis in South Africa: an assessment of the local evidence base. *S. Afr. Med. J.* 104: 174–177.
- Andrews, J. R., F. Noubary, R. P. Walensky, R. Cerda, E. Losina, and C. R. Horsburgh. 2012. Risk of progression to active tuberculosis following reinfection with *Mycobacterium tuberculosis*. *Clin. Infect. Dis.* 54: 784–791.
- Kaveh, D. A., V. S. Bachy, R. G. Hewinson, and P. J. Hogarth. 2011. Systemic BCG immunization induces persistent lung mucosal multifunctional CD4 T(EM) cells which expand following virulent mycobacterial challenge. *PLoS One* 6: e21566.
- Johnson, D. F., L. L. Malone, S. Zalwango, J. Mukisa Oketcho, K. A. Chervenak, B. Thiel, H. Mayanja-Kizza, C. M. Stein, W. H. Boom, and C. L. Lancioni, Tuberculosis Research Unit. 2014. Tuberculin skin test reversion following isoniazid preventive therapy reflects diversity of immune response to primary *Mycobacterium tuberculosis* infection. *PLoS One* 9: e96613.
- Carrara, S., D. Vincenti, N. Petrosillo, M. Amicosante, E. Girardi, and D. Goletti. 2004. Use of a T cell-based assay for monitoring efficacy of antituberculosis therapy. *Clin. Infect. Dis.* 38: 754–756.
- Chee, C. B., K. W. KhinMar, S. H. Gan, T. M. Barkham, M. Pushparani, and Y. T. Wang. 2007. Latent tuberculosis infection treatment and T-cell responses to *Mycobacterium tuberculosis*-specific antigens. *Am. J. Respir. Crit. Care Med.* 175: 282–287.
- Ribeiro, S., K. Dooley, J. Hackman, C. Loredo, A. Efron, R. E. Chaisson, M. B. Conde, N. Boechat, and S. E. Dorman. 2009. T-SPOT.TB responses during treatment of pulmonary tuberculosis. *BMC Infect. Dis.* 9: 23.
- Chiappini, E., F. Bonsignori, G. Mangone, L. Galli, R. Mazzantini, S. Sollai, C. Azzari, and M. de Martino. 2012. Serial T-SPOT.TB and QuantiFERON-TB-Gold In-Tube assays to monitor response to antitubercular treatment in Italian children with active or latent tuberculosis infection. *Pediatr. Infect. Dis. J.* 31: 974–977.
- Chiappini, E., F. Fossi, F. Bonsignori, S. Sollai, L. Galli, and M. de Martino. 2012. Utility of interferon- $\gamma$  release assay results to monitor anti-tubercular treatment in adults and children. *Clin. Ther.* 34: 1041–1048.
- Dhedra, K., A. Pooran, M. Pai, R. F. Miller, K. Lesley, H. L. Booth, G. M. Scott, A. N. Akbar, A. Zumla, and G. A. Rook. 2007. Interpretation of *Mycobacterium tuberculosis* antigen-specific IFN-gamma release assays (T-SPOT.TB) and factors that may modulate test results. *J. Infect.* 55: 169–173.
- Lee, S. W., C. T. Lee, and J. J. Yim. 2010. Serial interferon-gamma release assays during treatment of active tuberculosis in young adults. *BMC Infect. Dis.* 10: 300.
- Lee, S. W., S. H. Lee, and J. J. Yim. 2012. Serial interferon-gamma release assays after chemoprophylaxis in a tuberculosis outbreak cohort. *Infection* 40: 431–435.
- Johnson, J. L., H. Geldenhuys, B. A. Thiel, A. Toefy, S. Suliman, B. Pienaar, P. Chheng, T. Scriba, W. H. Boom, W. Hanekom, and M. Hatherill. 2014. Effect of isoniazid therapy for latent TB infection on QuantiFERON-TB gold in-tube responses in adults with positive tuberculin skin test results in a high TB incidence area: a controlled study. *Chest* 145: 612–617.
- Hatherill, M., H. Geldenhuys, B. Pienaar, S. Suliman, P. Chheng, S. M. Debanne, D. F. Hoft, W. H. Boom, W. A. Hanekom, and J. L. Johnson. 2014. Safety and reactivity of BCG revaccination with isoniazid pretreatment in TST positive adults. *Vaccine* 32: 3982–3988.
- Kagina, B. M., N. Mansoor, E. P. Kpamegan, A. Penn-Nicholson, E. Nemes, E. Smit, S. Gelderbloem, A. P. Soares, B. Abel, A. Keyser, et al. 2014. Qualification of a whole blood intracellular cytokine staining assay to measure mycobacteria-specific CD4 and CD8 T cell immunity by flow cytometry. *J. Immunol. Methods* 417: 22–33.
- Roederer, M., J. L. Nozzi, and M. C. Nason. 2011. SPICE: exploration and analysis of post-cytometric complex multivariate datasets. *Cytometry A* 79: 167–174.
- Li, Z., B. Yang, Y. Zhang, J. Ma, X. Chen, S. Lao, B. Li, and C. Wu. 2014. *Mycobacterium tuberculosis*-specific memory NKT cells in patients with tuberculous pleurisy. *J. Clin. Immunol.* 34: 979–990.
- Kleinnijenhuis, J., J. Quintin, F. Preijers, L. A. Joosten, C. Jacobs, R. J. Xavier, J. W. van der Meer, R. van Crevel, and M. G. Netea. 2014. BCG-induced trained immunity in NK cells: role for non-specific protection to infection. *Clin. Immunol.* 155: 213–219.
- Cooper, M. A., T. A. Fehniger, and M. A. Caligiuri. 2001. The biology of human natural killer-cell subsets. *Trends Immunol.* 22: 633–640.
- O'Sullivan, T. E., J. C. Sun, and L. L. Lanier. 2015. Natural killer cell memory. *Immunity* 43: 634–645.
- Sun, J. C., J. N. Beilke, and L. L. Lanier. 2009. Adaptive immune features of natural killer cells. *Nature* 457: 557–561.
- Horowitz, A., R. H. Behrens, L. Okell, A. R. Fooks, and E. M. Riley. 2010. NK cells as effectors of acquired immune responses: effector CD4+ T cell-dependent activation of NK cells following vaccination. *J. Immunol.* 185: 2808–2818.
- Penn-Nicholson, A., H. Geldenhuys, W. Burny, R. van der Most, C. L. Day, E. Jongert, P. Moris, M. Hatherill, O. Ofori-Anyinam, W. Hanekom, et al; Vaccine Study Team. 2015. Safety and immunogenicity of candidate vaccine M72/AS01E in adolescents in a TB endemic setting. *Vaccine* 33: 4025–4034.

28. Kupz, A., U. Zedler, M. Staber, C. Perdomo, A. Dorhoi, R. Brosch, and S. H. Kaufmann. 2016. ESAT-6-dependent cytosolic pattern recognition drives noncognate tuberculosis control in vivo. *J. Clin. Invest.* 126: 2109–2122.
29. Sun, J. C., S. Madera, N. A. Bezman, J. N. Beilke, M. H. Kaplan, and L. L. Lanier. 2012. Proinflammatory cytokine signaling required for the generation of natural killer cell memory. *J. Exp. Med.* 209: 947–954.
30. Abu-Raddad, L. J., L. Sabatelli, J. T. Achterberg, J. D. Sugimoto, I. M. Longini, Jr., C. Dye, and M. E. Halloran. 2009. Epidemiological benefits of more-effective tuberculosis vaccines, drugs, and diagnostics. *Proc. Natl. Acad. Sci. USA* 106: 13980–13985.
31. Scriba, T. J., B. Kalsdorf, D. A. Abrahams, F. Isaacs, J. Hofmeister, G. Black, H. Y. Hassan, R. J. Wilkinson, G. Walzl, S. J. Gelderbloem, et al. 2008. Distinct, specific IL-17- and IL-22-producing CD4+ T cell subsets contribute to the human anti-mycobacterial immune response. *J. Immunol.* 180: 1962–1970.
32. Andrews, J. R., M. Hatherill, H. Mahomed, W. A. Hanekom, M. Campo, T. R. Hawn, R. Wood, and T. J. Scriba. 2015. The dynamics of QuantiFERON-TB gold in-tube conversion and reversion in a cohort of South African adolescents. *Am. J. Respir. Crit. Care Med.* 191: 584–591.
33. Mangtani, P., I. Abubakar, C. Ariti, R. Beynon, L. Pimpin, P. E. Fine, L. C. Rodrigues, P. G. Smith, M. Lipman, P. F. Whiting, and J. A. Sterne. 2014. Protection by BCG vaccine against tuberculosis: a systematic review of randomized controlled trials. *Clin. Infect. Dis.* 58: 470–480.
34. Barreto, M. L., D. Pilger, S. M. Pereira, B. Genser, A. A. Cruz, S. S. Cunha, C. Sant'Anna, M. A. Hijjar, M. Y. Ichihara, and L. C. Rodrigues. 2014. Causes of variation in BCG vaccine efficacy: examining evidence from the BCG REVAC cluster randomized trial to explore the masking and the blocking hypotheses. *Vaccine* 32: 3759–3764.
35. Kagina, B. M., B. Abel, T. J. Scriba, E. J. Hughes, A. Keyser, A. Soares, H. Gamielidien, M. Sidibana, M. Hatherill, S. Gelderbloem, et al; other members of the South African Tuberculosis Vaccine Initiative. 2010. Specific T cell frequency and cytokine expression profile do not correlate with protection against tuberculosis after bacillus Calmette-Guérin vaccination of newborns. *Am. J. Respir. Crit. Care Med.* 182: 1073–1079.
36. Morita, D., Y. Hattori, T. Nakamura, T. Igarashi, H. Harashima, and M. Sugita. 2013. Major T cell response to a mycolyl glycolipid is mediated by CD1c molecules in rhesus macaques. *Infect. Immun.* 81: 311–316.
37. Van Rhijn, I., A. Kasmar, A. de Jong, S. Gras, M. Bhati, M. E. Doorenspleet, N. de Vries, D. I. Godfrey, J. D. Altman, W. de Jager, et al. 2013. A conserved human T cell population targets mycobacterial antigens presented by CD1b. *Nat. Immunol.* 14: 706–713.
38. Wheeler, P. R., and P. M. Anderson. 1996. Determination of the primary target for isoniazid in mycobacterial mycolic acid biosynthesis with *Mycobacterium aurum* A+. *Biochem. J.* 318: 451–457.
39. Kasmar, A. G., I. van Rhijn, T. Y. Cheng, M. Turner, C. Seshadri, A. Schiefner, R. C. Kalathur, J. W. Annand, A. de Jong, J. Shires, et al. 2011. CD1b tetramers bind  $\alpha\beta$  T cell receptors to identify a mycobacterial glycolipid-reactive T cell repertoire in humans. *J. Exp. Med.* 208: 1741–1747.
40. Schlums, H., F. Cichocki, B. Tesi, J. Theorell, V. Beziat, T. D. Holmes, H. Han, S. C. Chiang, B. Foley, K. Mattsson, et al. 2015. Cytomegalovirus infection drives adaptive epigenetic diversification of NK cells with altered signaling and effector function. *Immunity* 42: 443–456.
41. Lee, J., T. Zhang, I. Hwang, A. Kim, L. Nitschke, M. Kim, J. M. Scott, Y. Kamimura, L. L. Lanier, and S. Kim. 2015. Epigenetic modification and antibody-dependent expansion of memory-like NK cells in human cytomegalovirus-infected individuals. *Immunity* 42: 431–442.
42. Merle, C. S., S. S. Cunha, and L. C. Rodrigues. 2010. BCG vaccination and leprosy protection: review of current evidence and status of BCG in leprosy control. *Expert Rev. Vaccines* 9: 209–222.
43. Kleinnijenhuis, J., J. Quintin, F. Preijers, L. A. Joosten, D. C. Ifrim, S. Saeed, C. Jacobs, J. van Loenhout, D. de Jong, H. G. Stunnenberg, et al. 2012. Bacille Calmette-Guérin induces NOD2-dependent nonspiciferous protection from reinfection via epigenetic reprogramming of monocytes. *Proc. Natl. Acad. Sci. USA* 109: 17537–17542.
44. Lauwerys, B. R., J. C. Renaud, and F. A. Houssiau. 1999. Synergistic proliferation and activation of natural killer cells by interleukin 12 and interleukin 18. *Cytokine* 11: 822–830.
45. Soares, A. P., T. J. Scriba, S. Joseph, R. Harbacheuski, R. A. Murray, S. J. Gelderbloem, A. Hawkrigde, G. D. Hussey, H. Maecker, G. Kaplan, and W. A. Hanekom. 2008. *Bacillus Calmette-Guérin* vaccination of human newborns induces T cells with complex cytokine and phenotypic profiles. *J. Immunol.* 180: 3569–3577.
46. Zufferey, C., S. Germano, B. Dutta, N. Ritz, and N. Curtis. 2013. The contribution of non-conventional T cells and NK cells in the mycobacterial-specific IFN $\gamma$  response in Bacille Calmette-Guérin (BCG)-immunized infants. *PLoS One* 8: e77334.
47. Soares, A. P., C. K. Kwong Chung, T. Choice, E. J. Hughes, G. Jacobs, E. J. van Rensburg, G. Khomba, M. de Kock, L. Lerumo, L. Makhetha, et al. 2013. Longitudinal changes in CD4(+) T-cell memory responses induced by BCG vaccination of newborns. *J. Infect. Dis.* 207: 1084–1094.
48. Montaldo, E., C. Vitale, F. Cottalasso, R. Conte, T. Glatzer, P. Ambrosini, L. Moretta, and M. C. Mingari. 2012. Human NK cells at early stages of differentiation produce CXCL8 and express CD161 molecule that functions as an activating receptor. *Blood* 119: 3987–3996.
49. Ji, H. F., J. Wang, L. Yu, J. Q. Niu, D. A. Ayana, and Y. F. Jiang. 2013. High frequencies of CD158b+ NK cells are associated with persistent hepatitis C virus infections. *Ann. Hepatol.* 12: 539–547.
50. Nielsen, C. M., M. J. White, M. R. Goodier, and E. M. Riley. 2013. Functional significance of CD57 expression on human NK cells and relevance to disease. *Front. Immunol.* 4: 422.
51. World Health Organization. 2015. Guidelines on the Management of Latent Tuberculosis Infection. Available at: [http://apps.who.int/iris/bitstream/10665/136471/1/9789241548908\\_eng.pdf?ua=1&ua=1](http://apps.who.int/iris/bitstream/10665/136471/1/9789241548908_eng.pdf?ua=1&ua=1).